

# Improving the calibration process of inertial measurement unit for marine applications

Hossein Rahimi  | Amir Ali Nikkhah 

K. N. Toosi University of Technology

## Correspondence

Hossein Rahimi, K. N. Toosi University of Technology

Email: [h\\_rahimi@email.kntu.ac.ir](mailto:h_rahimi@email.kntu.ac.ir)

## Abstract

Marine navigation systems have very accurate sensors, such as 0.01deg/hr gyro drift stability and 0.1mg/year accelerometer bias stability. Common calibration methods and equipment do not meet the accuracy required. In this paper, a systematic method for calibration of an inertial measurement unit (IMU) for marine applications is proposed which is not based on the accuracy of the calibration turn table and only requires one specific plate to determine the initial attitude of the IMU and functions independently of the turn table. The first contribution of this paper is to derive a model for systematic calibration of IMU that expresses the rotation matrix error and velocity as a linear function of the calibration parameters at any time. As the second contribution, this paper proposes a calibration algorithm with only using an initial, specific plate. Using the actual data, it was found that the proposed algorithm provides a good estimation of the parameters.

## KEYWORDS

accelerometer, calibration, error model, gyroscope, inertial measurement unit, weighted least square

## 1 | INTRODUCTION

In recent years, with advances in the design and development of highly accurate optical and laser gyroscopes and precision accelerometers, a new family of highly accurate inertial navigation systems consisting of the types of sensors has been developed. This has led to major advances in inertial navigation technology and is now widely used in a variety of aerospace, marine, and land applications due to its superior performance and reasonable costs (Cai et al., 2016).

One of the most important issues in dealing with such accurate systems is the calibration and compensation of the inertial sensor error parameters. Calibration is a fundamental and indispensable process for the production and use of inertial navigation systems and is particularly important for accurate navigation systems. The purpose of calibration is to estimate the non-stochastic errors of the

IMU. The calibration results are used to compensate the raw outputs of IMU and thus to eliminate their repeatable errors (Kozlov et al., 2014).

Marine navigation systems are one of the systems which must be sufficiently accurate in harsh sea conditions. Due to the high dynamics of the sea, any small error in the calibration parameters of marine navigation systems causes a large error in the system outputs. Also, concerning marine navigation algorithms, matching the data of the accelerometer and gyroscope sensors is very important in the ultimate navigation accuracy. Matching between gyroscopes and accelerometers means creating a precise alignment between their axes in the calibration process. For example, the x-axis of the accelerometer is exactly parallel to the x-axis of the gyroscope. In separation-based calibration methods, this match usually does not happen well because the gyroscopes and accelerometers are calibrated independently. Given the sea conditions, the issue of the lever arm

effect on calibration is of great importance. High dynamics in marine applications mean continual oscillations due to swell and wind waves. Under sea conditions, inertial sensors are always subject to oscillating inputs and a small error in the bias or scale factor, due to the persistence of oscillations, causes a large error in attitude, velocity, and position.

Existing calibration methods are generally divided into two categories: conventional separation methods and systematic grade methods, each with its own advantages and disadvantages. In the conventional separation method, the calibration parameters are extracted directly from the sensors and comparing them with the desired values. In the separation-based calibration method, precise turn tables are usually used and the calibration accuracy depends on the accuracy of the turn table. In this method, to calibrate the accelerometers, the turn table is placed in different attitudes, and in each attitude, the output of the accelerometers are stored. Also, based on the amount of gravitational acceleration at the calibration location and the specified attitude of the turn table, the image of the gravitational acceleration on each IMU axis, in each attitude, is calculated. Accelerometer calibration parameters are calculated from the average output of the accelerometers along with the image values of the gravitational acceleration in each attitude using methods such as the minimum least square error. The desired values in the accelerometer calibration are the images of the gravitational acceleration in each attitude. To calculate the calibration parameters of gyroscopes, certain angular velocities are applied to the turn table at different axes, and in this case, the output of the gyroscopes are stored. From the average output of the gyroscopes at each angular velocity as well as the amount of angular velocity that applied to the turn table, the calibration parameters of the gyroscopes are calculated using methods such as the minimum least square error. The desired values in the calibration of gyroscopes are the angular velocities applied to the turn table. Systematic grade methods are based on solving the navigation equations assuming zero velocity and the fixed position. The separation calibration method is simpler but requires stricter test conditions and more sophisticated instruments. In contrast, the systematic grade calibration methods do not require very precise equipment and are more suitable for practical applications. However, the disadvantages of the systematic grade methods are the existence of complicated and tedious computations, difficult observation analysis, and longer calibration time due to the use of conventional error estimation filters (Cai et al., 2016).

In all studies on system grade calibration of IMU, stochastic dynamics models and stochastic filters have been used (Cai et al., 2016; Kozlov et al., 2013, 2014; Pan et al., 2014; Vavilova and Sazonov, 2012). Most of these

face the problem of observability and convergence because the calibration parameters are constant values without dynamics. Because of the limited observability, it is necessary to apply a specific movement to the system to determine each calibration parameter to make that parameter more observable. In Xie et al. (2010), the system grade method was considered based on the Kalman filter with fifty-one states. These states include the attitude error, velocity, position, and calibration parameters. The dynamic model considered in this reference is the usual linearized navigation error model. The only measurement used in the model is velocity. For the calibration parameters, the dynamic model is assumed to have constant values (derivative equal to zero), and due to the difficulty of observing the parameters, the movements are applied to the turn table. In this reference, there is no definition of the axes of the IMU, and it is possible to rotate the axes relative to the body of the system during the calibration process. Cai et al. (2016) proposed a method for the calibration of navigation systems with optical sensors by using inaccurate calibration turn tables. This reference does not address non-orthogonal parameters for the x-axis accelerometer, and this axis is considered as the x-axis of the system in the calibration process. In this reference, the linearized model of navigation error dynamics in the Kalman filter is applied using velocities as measurements. Also, in the method proposed in this reference, certain movements have been used for proper convergence. In Kozlov et al. (2014) and Parusnikov (2009), a systematic calibration method was developed for the specific dynamics of a navigation system based on the Kalman filter.

In Hung and Lee, (2006), a Calibration method based on high accuracy turn table for the six accelerometer IMU is described. In Shin & El-Sheimy (2002) and Salychev (1998), the Local Level Frame (LLF) method is described. In this calibration method, IMUs are being mounted on a multi-axis turn table whose axes are precisely aligned with the LLF. The unit is then rotated through a series of known exact angles and placed in different directions according to the LLF. This method of calibration has two main drawbacks: a) The magnitude of the Earth's rotation usually leads to a problem in estimating gyro biases. b) The need for IMU axis alignment according to LLF (Shin & El-Sheimy, 2002). In Shin & El-Sheimy (2002) and Rogers (2007), the Six Position Static Acceleration Calibration method is described. In this calibration method, the IMU is installed on a turn table, with each sensitive axis pointing up and down alternately (six positions). Therefore, estimates of accelerometer bias and scale factor can be extracted by summing and differencing combinations of the inertial system measurements. The limitations of this method are that non-orthogonality cannot be determined, and that the misalignment of the IMU sensitive

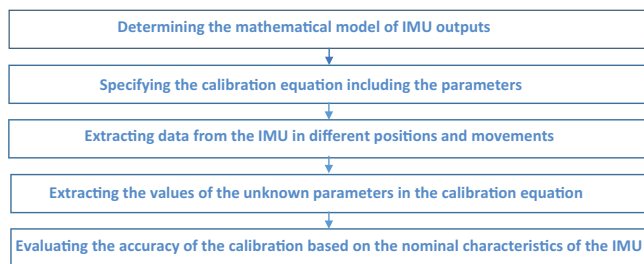


**FIGURE 1** Calibration implementation flowchart [Color figure can be viewed in the online issue, which is available at [wileyonlinelibrary.com](http://wileyonlinelibrary.com) and [www.ion.org](http://www.ion.org)]

axes under investigation with respect to the vertical direction can affect the result even though it is very small (Shin & El-Sheimy, 2002). In Hayal (2010), Syed et al. (2007), and Zhang et al. (2008), the Multi-position Calibration method is described. In this calibration method, take the Earth's rotation rate and gravity as inputs, and calculate the calibration parameters based on two facts: 1) the norm of the accelerometer measurement vector is equal to the gravity; 2) the dot product of the gyroscope measurement vector and the accelerometer measurement vector is equal to the negative dot product of the Earth's rotation and the Earth's gravity (Syed et al., 2007). In Li et al. (2011), the Multi-position Calibration method is used for calibration of a dynamically tuned gyroscope. The limitation of this method is that the non-orthogonality cannot be accurately determined. In Nieminen et al. (2010) and Särkkä et al. (2017), the Standard Multi-position Calibration method is described. In this calibration method, the standard multi-position calibration algorithm for consumer-grade IMUs using a rate table is enhanced to also exploit the centripetal accelerations caused by the rotation of the table (Nieminen et al., 2010). The limitation of this method is the same as the Multi-position Calibration method.

To calibrate an IMU, five steps must be taken, shown in Figure 1. In the first step, the mathematical model of the sensor output (generally, the IMU) is determined. To extract this model, a good understanding of the sensor is required. Sensitivity and behavior of the output to different input factors must be specified. In the second step, the calibration equation, including the parameters, needs to be specified. For example, for an IMU in the navigation class under normal conditions, the main parameters may include bias, scale factors, and non-orthogonality. The third step is to extract data from the IMU in different positions and movements. At this step, the IMU is first placed on the calibration turn table. Next, in order to estimate the calibration parameters, predetermined movements are applied to the table, and the IMU's output data is stored. In the fourth step, the values of the unknown parameters in the calibration equation are extracted. At this step, by

determining the measured values, the desired values, and the parametric calibration equation, unknown parameters can be obtained by system identification methods such as the least squares and stochastic filter-based methods. In the fifth step, the accuracy of the calibration is evaluated based on the nominal characteristics of the IMU. This evaluation is usually done with data collected during the calibration process and additional data. In order to evaluate the validation of the calibration, different methods can be used based on the accuracy of the calibration turn table. In methods such as separation, which are based on the accuracy of the turn table, the turn table can be rotated, and the calibrated output of the sensors can be compared to the values of angular velocity applied to the turn table or to the amount of the gravitational acceleration image on each IMU axis. In methods such as systematic grade calibration, which are not based on the turn table accuracy, velocities are usually used as a measure of calibration accuracy. In these criteria, the calibrated sensors data are usually stored during the rotation of the turn table, then the turn table stops in an attitude. Now, these calibrated sensors data are used in navigation equations, and the desired values of velocities are zero after the end of the rotation. That is, due to the lack of positional displacement of the set, the desired velocities are zero, and the calibration error is measured on this basis.

This paper focuses on systematic grade calibration methods and proposes a method in which inaccurate test equipment and turn tables are used for the calibration of precision IMU. Marine navigation systems usually have very accurate sensors. Conventional calibration methods and equipment do not meet the accuracy required. This paper presents a systematic method for calibration of an IMU for marine navigation applications. The assumption of calibration specificity for marine navigation is because the IMU movements during the calibration process are considered following the sea turbulence model.

Our proposed method is based on systematic calibration. Stochastic filters are used in existing systematic methods. In this case, we have three problems:

1. The calibration coefficients are non-dynamic; all of the dynamic matrix coefficients used for the stochastic filters are zero. This means that the stochastic filters do not work properly. A non-dynamic or low-dynamic stochastic filter is practically like a recursive least square method.
2. In all stochastic filter-based methods, it is necessary to consider the attitude errors as a filter state. In other words, in addition to estimating the error of the sensors, the filter must also have an estimate of the error of the attitude. That is, the part of the correction that should be related to the sensors is done in the attitude.

3. In the calibration of precision IMUs, the calibration axes are very important, and the axes must be in accordance with the mechanical indicators. In systematic methods based on stochastic filters, it is always possible to rotate the calibration axes relative to the mechanical index axes. In conventional systematic calibrations, the matching between the calibration axes and the mechanical indicators of the IMU usually does not occur.

The first contribution of this paper is to derive a model for the systematic calibration of IMU that expresses the rotation matrix error and velocity as a linear function of the calibration parameters at any time. Now, if at any point in time the exact values of velocity are known, the calibration parameters can be estimated using methods such as least square. Due to this innovation, it is possible to use batch data in the least squares error method, while methods based on stochastic filters behave similarly to the recursive square method (dynamic matrix arrays due to calibration coefficients are zero). Batch-based methods always have a more accurate estimate of recursive methods. Also, based on the proposed innovations, unlike stochastic filter-based methods, only calibration coefficients are estimated. In other words, in the proposed method, all errors are related to correction in calibration coefficients. While in stochastic filter-based methods, part of the error is related to changing the attitude.

As the second contribution, this paper proposes a calibration algorithm by only using an initial, specific attitude. The proposed calibration method is superior to the separation-based methods, whose accuracy is always based on the accuracy of the turn table, since it requires precision only in an initial attitude. Also, due to the fact that in the proposed algorithm the initial attitude is determined according to the mechanical indicators, the calibration axes are always matched to the mechanical index axes, and no error occurs in this case. However, in stochastic filter-based methods, it is always possible to rotate the calibration axes relative to the mechanical index axes. In conventional systematic calibrations, the matching between the calibration axes and the mechanical indicators of the IMU usually does not occur. This creates an error in the use of the IMU after the calibration process in precise applications.

The rest of this paper is organized into seven sections. In the second section, the calibration equation used in the IMU is expressed. In the third section, the linear error model is extracted. In the fourth section, the measurement values are specified. In the fifth section, the equations used for extracting the parameters are present. In the sixth section, the proposed method is implemented for an inertial measurement system, and the validity of the algorithm and the extracted parameters are evalu-

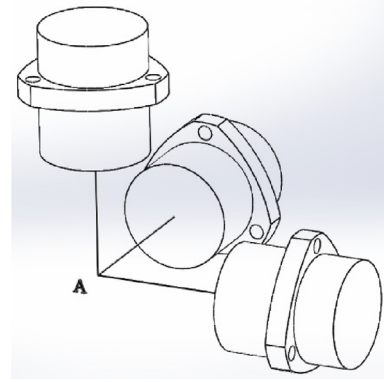


**FIGURE 2** Accelerometers lever arm effect [Color figure can be viewed in the online issue, which is available at [wileyonlinelibrary.com](http://wileyonlinelibrary.com) and [www.ion.org](http://www.ion.org)]

ated. Finally, the conclusion is presented in the seventh section.

## 2 | THE CALIBRATION EQUATION OF THE IMU

Because the purpose of this paper is to calibrate a precise IMU based on Q-Flex accelerometers and FOG gyroscopes and based on the specifications of the desired IMU, the general calibration model is developed based on a number of parameters including bias, scale factors, non-orthogonality, and the lever arm effect for accelerometers and the second-order effects of angular velocity in gyroscopes. Accordingly, for accelerometers, we have

$$\begin{bmatrix} a_{xc} \\ a_{yc} \\ a_{zc} \end{bmatrix} = \begin{bmatrix} S_x^{acc} & m_{xy}^{acc} & m_{xz}^{acc} \\ m_{yx}^{acc} & S_y^{acc} & m_{yz}^{acc} \\ m_{zx}^{acc} & m_{zy}^{acc} & S_z^{acc} \end{bmatrix} \begin{bmatrix} a_{xr} \\ a_{yr} \\ a_{zr} \end{bmatrix} + \begin{bmatrix} a_x^{bias} \\ a_y^{bias} \\ a_z^{bias} \end{bmatrix} + \begin{bmatrix} r_x & 0 & 0 \\ 0 & r_y & 0 \\ 0 & 0 & r_z \end{bmatrix} \begin{bmatrix} \omega_{yc}^2 + \omega_{zc}^2 \\ \omega_{xc}^2 + \omega_{zc}^2 \\ \omega_{xc}^2 + \omega_{yc}^2 \end{bmatrix}, \quad (1)$$

where  $S$  represents the scale factor,  $m$  is the non-orthogonality, and  $r$  shows the parameters related to the lever arm effect. The accelerometer sensitive axes intersect at the measurement point of IMU (point A) in Figure 2. The distance from the mounting position of each accelerometer to the origin is called the lever arm.

In general, the acceleration due to the lever arm effect on each accelerometer is calculated as follows (Salychev, 2004):

$$a^{LA} = -W \times (W \times R), \quad (2)$$

where  $W$  is the angular velocity vector,  $R$  is the vector of the acceleration distance from the vertex, and  $\times$  is the cross-product operator. In the case that each accelerometer is just away from the vertex in across its own axel, the overall acceleration equation obtained by the lever arm effect for the three accelerometers is simplified as follows:

$$\begin{bmatrix} a_x^{LA} \\ a_y^{LA} \\ a_z^{LA} \end{bmatrix} = \begin{bmatrix} r_x & 0 & 0 \\ 0 & r_y & 0 \\ 0 & 0 & r_z \end{bmatrix} \begin{bmatrix} \omega_{yc}^2 + \omega_{zc}^2 \\ \omega_{xc}^2 + \omega_{zc}^2 \\ \omega_{xc}^2 + \omega_{yc}^2 \end{bmatrix}. \quad (3)$$

Equation (3) can be rewritten as follows:

$$\begin{bmatrix} a_{xc} \\ a_{yc} \\ a_{zc} \end{bmatrix} = \begin{bmatrix} S_x^{acc} & m_{xy}^{acc} & m_{xz}^{acc} & a_x^{bias} & r_x & 0 & 0 \\ m_{yx}^{acc} & S_y^{acc} & m_{yz}^{acc} & a_y^{bias} & 0 & r_y & 0 \\ m_{zx}^{acc} & m_{zy}^{acc} & S_z^{acc} & a_z^{bias} & 0 & 0 & r_z \end{bmatrix} \times \begin{bmatrix} a_{xr} \\ a_{yr} \\ a_{zr} \\ 1 \\ \omega_{yc}^2 + \omega_{zc}^2 \\ \omega_{xc}^2 + \omega_{zc}^2 \\ \omega_{xc}^2 + \omega_{yc}^2 \end{bmatrix}. \quad (4)$$

And we define

$$\begin{bmatrix} S_x^{acc} & m_{xy}^{acc} & m_{xz}^{acc} & a_x^{bias} & r_x & m_{yx}^{acc} & S_y^{acc} & m_{yz}^{acc} & a_y^{bias} & r_y & m_{zx}^{acc} \\ (m_{zy}^{acc} & S_z^{acc} & a_z^{bias} & r_z)^T \end{bmatrix} \approx k^{acc} + \delta k^{acc}, \quad (5)$$

where  $k^{acc}$  is the initial calibration parameter value of the accelerometers and  $\delta k^{acc}$  is the calibration parameter error.

For gyroscopes, we have

$$\begin{bmatrix} \omega_{xc} \\ \omega_{yc} \\ \omega_{zc} \end{bmatrix} = \begin{bmatrix} S_x^{gyro} & m_{xy}^{gyro} & m_{xz}^{gyro} \\ m_{yx}^{gyro} & S_y^{gyro} & m_{yz}^{gyro} \\ m_{zx}^{gyro} & m_{zy}^{gyro} & S_z^{gyro} \end{bmatrix} \begin{bmatrix} \omega_{xr} \\ \omega_{yr} \\ \omega_{zr} \end{bmatrix} + \begin{bmatrix} \omega_x^{bias} \\ \omega_y^{bias} \\ \omega_z^{bias} \end{bmatrix} + \begin{bmatrix} e_x & 0 & 0 \\ 0 & e_y & 0 \\ 0 & 0 & e_z \end{bmatrix} \begin{bmatrix} \omega_{xr}^2 \\ \omega_{yr}^2 \\ \omega_{zr}^2 \end{bmatrix}, \quad (6)$$

where  $S$  represents the scale factor,  $m$  is the non-orthogonality, and  $r$  shows the parameters related to the second-order effect. Equation (5) can be rewritten as follows:

$$\begin{bmatrix} \omega_{xc} \\ \omega_{yc} \\ \omega_{zc} \end{bmatrix} = \begin{bmatrix} S_x^{gyro} & m_{xy}^{gyro} & m_{xz}^{gyro} & \omega_x^{bias} & e_x & 0 & 0 \\ m_{yx}^{gyro} & S_y^{gyro} & m_{yz}^{gyro} & \omega_y^{bias} & 0 & e_y & 0 \\ m_{zx}^{gyro} & m_{zy}^{gyro} & S_z^{gyro} & \omega_z^{bias} & 0 & 0 & e_z \end{bmatrix}$$

$$\times \begin{bmatrix} \omega_{xr} \\ \omega_{yr} \\ \omega_{zr} \\ 1 \\ \omega_{xr}^2 \\ \omega_{yr}^2 \\ \omega_{zr}^2 \end{bmatrix}. \quad (7)$$

And we define

$$\begin{bmatrix} S_x^{gyro} & m_{xy}^{gyro} & m_{xz}^{gyro} & \omega_x^{bias} & e_x & m_{yx}^{gyro} & S_y^{gyro} & m_{yz}^{gyro} & \omega_y^{bias} & e_y \\ m_{zx}^{gyro} & m_{zy}^{gyro} & S_z^{gyro} & \omega_z^{bias} & e_z \end{bmatrix}^T \approx k^{gyro} + \delta k^{gyro}, \quad (8)$$

where  $k^{gyro}$  is the initial calibration parameter value of the gyroscopes and  $\delta k^{gyro}$  is the calibration parameter error. The purpose of improving the calibration process is to estimate the calibration error parameters  $\delta k^{gyro}$  and  $\delta k^{acc}$ .

In various papers that have used systematic grade methods for calibration, the x-axis of the accelerometer in the IMU is usually used as a reference, and the calibration axes are formed based on it. Accordingly, in the calibration equations, the non-orthogonality parameters for the x-axis are considered to be zero compared to other axes. This means that the x-axis accelerometer does not have non-orthogonality, and its axes are considered correct as the x-axis of the calibration. This does not always produce the right results. In situations where the x-axis corresponding to the IMU is used as the calibration axis, if this axis does not conform to the mechanical indicators on the IMU, the results in using the IMU may not always be correct. In the calibration process, we usually want to set the axes of the IMU based on the references specified on the IMU mechanics. This is considered in the proposed method, and the calibration is generally based on the mechanical indexes of the IMU.

### 3 | THE ERROR MODEL

Because our goal in calibration is not to use stochastic filters, only the deterministic parameters are considered in this model. In general, the calibrated output of the gyroscopes is the angular velocity of the body frame relative to the inertial frame in the body frame ( $\omega_{ib}^b$ ). This angular velocity is the sum of the following three angular velocities (Titterton et al., 2004):

$$\omega_{ib}^b = \omega_{ie}^b + \omega_{en}^b + \omega_{nb}^b, \quad (9)$$

where  $\omega_{en}^b$  is the transport rate, which is zero in our application due to the lack of spatial displacement of the



system in the calibration process. Also,  $\omega_{ie}^b$  is the effect of the angular velocity of the Earth on the body system. Given the differential equations of the rotation matrix, we have (Titterton et al., 2004)

$$\dot{C}_b^n = C_b^n \Omega_{nb}^b, \quad (10)$$

where  $C_b^n$  is the transformation matrix from the body frame to the navigation frame,  $\dot{C}_b^n$  is the update of  $C_b^n$ , and  $\Omega_{nb}^b$  is the skew symmetric matrix of  $\omega_{nb}^b$  and is written as follows:

$$\Omega_{nb}^b = \begin{bmatrix} 0 & -\omega_{nbz}^b & \omega_{nbx}^b \\ \omega_{nbz}^b & 0 & -\omega_{nby}^b \\ -\omega_{nbx}^b & \omega_{nby}^b & 0 \end{bmatrix}. \quad (11)$$

Given the angular velocity equality in Equation (9) and related to the zero-transport rate, we have

$$\begin{aligned} \Omega_{nb}^b &= \Omega_{ib}^b - \Omega_{ie}^b \\ \dot{C}_b^n &= C_b^n (\Omega_{ib}^b - \Omega_{ie}^b) C_b^n \Omega_{ib}^b C_b^n \Omega_{ie}^b C_b^n C_b^n \Omega_{ib}^b \Omega_{ie}^b C_b^n. \end{aligned} \quad (12)$$

Assuming the error due to the calibration correction parameters is insignificant, the rotation matrix can be written as a sum of two rotation matrices generated from the initial calibration parameters and the corrected calibration parameters:

$$\begin{aligned} C_b^n &= \tilde{C}_b^n + \delta C_b^n \\ \Omega_{ib}^b &= \tilde{\Omega}_{ib}^b + \delta \Omega_{ib}^b. \end{aligned} \quad (13)$$

By replacing the values obtained from Equation (13) into Equation (12), and given that the Earth's angular velocity at the calibration site is specified, we have

$$\dot{C}_b^n + \delta \dot{C}_b^n = (\tilde{C}_b^n + \delta C_b^n)(\tilde{\Omega}_{ib}^b + \delta \Omega_{ib}^b) - \Omega_{ie}^n (\tilde{C}_b^n + \delta C_b^n). \quad (14)$$

By multiplying the values obtained from Equation (14), and eliminating the multiplication error, we have

$$\begin{aligned} \dot{C}_b^n + \delta \dot{C}_b^n &= \tilde{C}_b^n \tilde{\Omega}_{ib}^b + \tilde{C}_b^n \delta \Omega_{ib}^b + \delta C_b^n \tilde{\Omega}_{ib}^b - \Omega_{ie}^n \tilde{C}_b^n - \Omega_{ie}^n \delta C_b^n. \end{aligned} \quad (15)$$

Accordingly, we can write

$$\delta \dot{C}_b^n = \tilde{C}_b^n \delta \Omega_{ib}^b + \delta C_b^n \tilde{\Omega}_{ib}^b - \Omega_{ie}^n \delta C_b^n. \quad (16)$$

Equation (16) shows the variations in the rotation matrix error resulting from the error of the angular velocity image,

the angular velocity error themselves, and the Earth's angular velocity image error. Because the attitude of the IMU is completely clear at the first moment, the initial rotation matrix is also completely clear. In this case, because the rotation matrix and its error are considered to be summative, the rotation error matrix ( $\delta C_b^n(0)$ ) is considered to be zero, and the initial rotation matrix is the same as the initial attitude of the IMU (without error) and  $C_b^n(0) = 0_{3 \times 3}$ . By specifying the initial value of the rotation matrix error (assumed to be zero), the error value can be calculated as a function of the calibration error of the sensors ( $\delta \Omega_{ib}^b$ ) at any point in time. The velocity equation in the navigation system is written as follows (Gu et al., 2008):

$$\dot{V}^n = C_b^n f^b + g^n - (2\omega_{ie}^n + \omega_{en}^n) \times V^n. \quad (17)$$

Given the non-displacement of the IMU during the calibration process, by eliminating the transport rate, the velocity equation in the navigation system is simplified as follows:

$$\dot{V}^n = C_b^n f^b + g^n - 2\Omega_{ie}^n V^n, \quad (18)$$

where  $g^n$  is the gravitational acceleration in the geosystem, whose value at the calibration site is fully specified. The calibrated acceleration of the accelerometers is the sum of the acceleration calculated with the initial calibration parameters and the modified calibration parameters. Also, assuming the calibration error is insignificant, the velocity derivative can be written as the sum of a binomial equation as follows:

$$\begin{aligned} \dot{V}^n &= \dot{V}^n + \delta \dot{V}^n \\ f^b &= \tilde{f}^b + \delta f^b. \end{aligned} \quad (19)$$

By replacing the values obtained from Equation (19) into Equation (18), we have

$$\begin{aligned} \dot{V}^n + \delta \dot{V}^n &= (\tilde{C}_b^n + \delta C_b^n) (\tilde{f}^b + \delta f^b) \\ &+ g^n - 2\Omega_{ie}^n (\tilde{V}^n + \delta V^n). \end{aligned} \quad (20)$$

By multiplying the values in Equation (20), and based on Equation (18), we have

$$\begin{aligned} \dot{V}^n + \delta \dot{V}^n &= \delta C_b^n \tilde{f}^b + \delta C_b^n \delta f^b + \tilde{C}_b^n \delta f^b - 2\Omega_{ie}^n \delta V^n \\ &+ (\tilde{C}_b^n \tilde{f}^b + g^n - 2\Omega_{ie}^n \tilde{V}^n) \\ \dot{V}^n &= (\tilde{C}_b^n \tilde{f}^b + g^n - 2\Omega_{ie}^n \tilde{V}^n) \\ \delta \dot{V}^n &= \delta C_b^n \tilde{f}^b + \delta C_b^n \delta f^b + \tilde{C}_b^n \delta f^b - 2\Omega_{ie}^n \delta V^n. \end{aligned} \quad (21)$$

Assuming that the multiplication value of the two errors is insignificant and thus negligible, we arrive at

Equation (22):

$$\delta \dot{V}^n = \delta C_b^n \tilde{f}^b + \tilde{C}_b^n \delta f^b - 2 \Omega_{ie}^n \delta V^n. \quad (22)$$

According to Equation (22), the variations in the velocity error are due to the accelerometer output error, the error of transferring acceleration from the body frame to the navigation frame, and the error in Coriolis acceleration due to the velocity error. Assuming the initial velocity error is zero, one can derive the velocity error ( $\delta V^n$ ) at any point in time as a linear function of the acceleration error ( $\delta f^b$ ) and the rotation matrix error ( $\delta C_b^n$ ). By the discretization of Equations (16) and (22), Equation (23) is obtained, which can be solved recursively at any point in time, where  $\Delta t$  is the time interval.

$$\begin{aligned} \delta C_{b,j+1}^n &= \delta C_{b,j}^n + \Delta t \left( \tilde{C}_{b,j+1}^n \delta \Omega_{ib,j+1}^b + \delta C_{b,j}^n \tilde{\Omega}_{ib,j+1}^b \right. \\ &\quad \left. - \Omega_{ie}^n \delta C_{b,j}^n \right) \\ \delta V_{j+1}^n &= \delta V_j^n + \Delta t \left( \delta C_{b,j+1}^n \tilde{f}_{j+1}^b + \tilde{C}_{b,j+1}^n \delta f_{j+1}^b \right. \\ &\quad \left. - 2 \Omega_{ie}^n \delta V_j^n \right). \end{aligned} \quad (23)$$

Initial values of the velocity error and rotation matrix error are considered to be zero. The important point about the Equation (23) error equations stated above is that the rotation matrix and velocity error values for each rotation are expressed as a linear function of the calibration parameters, which is the essential point in the continuation of the calibration process:

$$\begin{aligned} \delta C_{b,j+1}^n &= L_1 \left( \delta C_{b,j}^n, \delta \Omega_{ib,j+1}^b \right) = L_2 \left( \delta \Omega_{ib,j+1}^b \right) \\ &= L_3 (\delta k^{gyro}) \\ \delta V_{j+1}^n &= L_4 \left( \delta C_{b,j+1}^n, \delta f_{j+1}^b \right) = L_5 \left( \delta \Omega_{ib,j+1}^b, \delta f_{j+1}^b \right) \\ &= L_6 (\delta k^{gyro}, \delta k^{acc}), \end{aligned} \quad (24)$$

where  $L_i$  shows a linear function. Also,  $\delta k^{gyro}$  and  $\delta k^{acc}$  are the correction of the calibration parameters of gyroscopes and accelerometers, where the calibration aims to estimate these parameters. Equation (24) can also be expressed as follows:

$$\begin{aligned} \delta C_b^n &= \sum_{n=1}^{15} \alpha_n \delta k_n^{gyro} + \sum_{n=1}^{15} 0 \delta k_n^{acc} \\ \delta V^n &= \sum_{n=1}^{15} \gamma_n \delta k_n^{gyro} + \sum_{n=1}^{15} \beta_n \delta k_n^{acc}, \end{aligned} \quad (25)$$

where  $\alpha_n$ ,  $\beta_n$ , and  $\gamma_n$  are specified as numerical arrays that are determined during the execution of each sensor dataset

in the calibration algorithm. Given that the rotation matrix has nine arrays and the velocity matrix has three arrays, we have

$$\begin{bmatrix} \delta C_b^n \\ \delta V^n \end{bmatrix}_{12 \times 1} = \begin{bmatrix} \alpha_{9 \times 15} & 0_{9 \times 15} \\ \gamma_{3 \times 15} & \beta_{3 \times 15} \end{bmatrix} \begin{bmatrix} \delta k^{gyro} \\ \delta k^{acc} \end{bmatrix}_{30 \times 1}. \quad (26)$$

Equation (26) is a linear and specific equation for errors in terms of the calibration parameters.

It should be noted that since there have been some simplifications in the model extraction, it is necessary to slowly converge the calibration parameters in the implementation of the algorithm so that the skipped values slowly become zero.

## 4 | THE MEASUREMENT VALUES

In the calibration data extraction process, it is assumed that the system will move from a completely specific state and eventually return to the same state. As a result, the initial rotation matrixes are completely clear (the accuracy is within our calibration requirements). Also, the velocity values at the beginning and end of the movements are zero. According to the said process, the error values of the rotation matrix and velocity at the beginning of the movement are zero, since the attitude and velocity are clear. Also, the desired values of the rotation matrix at the end of the movement are quite clear. Given that the initial conditions of the attitude and velocity are known and the navigation equations were solved during the movement using the initial calibration parameters, the rotation matrix and velocity values are obtained at the end of the path. By subtracting these values from the desired rotation matrix and velocity values, the measurement vector is obtained. Assuming the state error values are insignificant, the rotation matrix error is considered to be equal to the difference between two rotation matrices.

$$Z = \begin{bmatrix} \delta C_b^n \\ \delta V^n \end{bmatrix}_{Measure} = \begin{bmatrix} C_b^n \\ V^n \end{bmatrix}_{Navigation} - \begin{bmatrix} C_b^n \\ V^n \end{bmatrix}_{Actual}. \quad (27)$$

Section 5 explains that returning to the previous attitude with great precision is not a requirement for the proposed calibration algorithm. In cases where inaccurate turn tables are used, only velocities can be used as a measurement.

## 5 | PARAMETER CALCULATION

To calculate the calibration parameters, the weighted least squares (WLS) method is used. Since the variations in the rotation matrix error are smaller compared to the

velocity error, the weighting is used to balance the error convergence. However, if the velocity convergence is more important (which usually is so because the velocity convergence also involves angles convergence), weighting can be skipped. In the above equation, only the values of the calibration parameters are unknown. If we have  $m$  number of datasets, Equation (26) is applied to each dataset. If we put  $m$  number of equations in a row, then we have

$$\begin{bmatrix} \delta C_b^n \\ \delta V^n \\ \vdots \end{bmatrix}_{12m \times 1}^{Measure} = \begin{bmatrix} \alpha_{9 \times 15} & 0_{9 \times 15} \\ \gamma_{3 \times 15} & \beta_{3 \times 15} \\ \vdots & \vdots \end{bmatrix}_{12m \times 30} \begin{bmatrix} \delta k^{gyro} \\ \delta k^{acc} \end{bmatrix}_{30 \times 1}. \quad (28)$$

Therefore, given the least squares equation, we have

$$\begin{bmatrix} \delta k^{gyro} \\ \delta k^{acc} \end{bmatrix} = \left( \begin{bmatrix} \alpha_{9 \times 15} & 0_{9 \times 15} \\ \gamma_{3 \times 15} & \beta_{3 \times 15} \\ \vdots & \vdots \end{bmatrix}^T \begin{bmatrix} \alpha_{9 \times 15} & 0_{9 \times 15} \\ \gamma_{3 \times 15} & \beta_{3 \times 15} \\ \vdots & \vdots \end{bmatrix} \right)^{-1} \times \begin{bmatrix} \alpha_{9 \times 15} & 0_{9 \times 15} \\ \gamma_{3 \times 15} & \beta_{3 \times 15} \\ \vdots & \vdots \end{bmatrix}^T \begin{bmatrix} \delta C_b^n \\ \delta V^n \\ \vdots \end{bmatrix}. \quad (29)$$

Accordingly, the values of the calibration parameters are determined.

In cases where it is possible to return to the original attitude with good accuracy, the weight of the rotation matrix in estimating coefficients (using the least squares error method) can be considered large. In situations where the accuracy of the return to the initial attitude is not good (inaccurate turn table is used), the weight of the rotation matrix can be reduced, so that only the velocities (zeroing the velocities in navigation frame on all turn tables is possible) can be used as a measurement. If only the velocities are used as a measurement, the need for a precise return to the original attitude will be eliminated, and this process can be done with inaccurate turn tables.

## 6 | THE PROCESS EVALUATION USING REAL DATA

To evaluate the proposed algorithm, an IMU, with FOG gyroscopes and Q-FLEX accelerometers with the Table 1 accuracy characteristics and Figure 12 structure, is used.

The correctness and improvement of the results, except for the convergence of coefficients, has been examined in two methods. In the first method, the velocity error results are checked using the same data used in calibration or additional data. Given that there is no physical displacement at the time of data collection, we expect the veloc-

TABLE 1 Parameters values for IMU error model

Parameters values for accelerometers error model	
Fixed bias	100 $\mu g$
Velocity random walk	0.05 $m/s/\sqrt{h}$
Scale factor error	50 $ppm$
Input axis misalignment	10 $arc\ sec$
Parameters values for gyroscopes error model	
Fixed drift	0.01 $deg/hr$
Angular random walk (ARW)	0.01 $deg/\sqrt{h}$
Scale factor error	20 $ppm$
Input axis misalignment	5 $arc\ sec$

ity to be zero and its value not to increase over time. This parameter has also been used to compare the improvement in calibration parameters. In the second method, which is used for parameters such as the lever arm, the convergent results in the algorithm are compared with the design values. Based on the mechanical design of the accelerometer placements, the lever arm parameters can be measured. The accuracy of parameters, such as the lever arm, was assessed and confirmed by measuring the physical distance and comparing it to the results of the algorithm. Also, during data collection time, when the set is completely stationary, the average magnitude of acceleration data and angular velocity can be used to check the accuracy of calibration. In this case, these measurements are compared with the magnitude of the Earth's gravitational acceleration at the test position and the magnitude of the Earth's angular velocity.

The initial calibration was performed by a separation method with a calibration turn table with a precision of one arc minute. Besides, initial bias parameters, initial scale factor, and initial non-orthogonality for the sensors in the system were extracted. A precise status is determined for the beginning of the movements. This specific plate can be created by using hand-held turn tables that can be locked mechanically, or this specific status can be created by using a precision alignment plate. The system is in this exact state before the start and end of data capture for each dataset. The accuracy of the alignment plate is very important because the initial condition of the navigation equations, the final navigation error, and the system axes in the calibration are based on comparison with the accuracy of this plate. Since the equations are extracted with the assumption that the error values are small, we consider the data capture time for each dataset to be relatively short. Each dataset is less than one minute with a sampling rate of 100 times per second. With different moves applied to the IMU, 30 raw datasets are stored from the system. The values of the angle errors with the initial calibration parameters are shown in Figure 3.



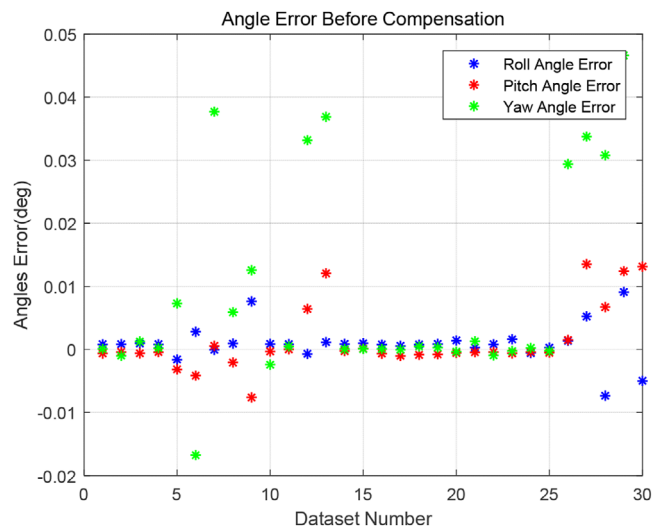


**FIGURE 3** Attitude error with initial calibration parameters at the end of the navigation process for 30 datasets each with three angles [Color figure can be viewed in the online issue, which is available at [wileyonlinelibrary.com](http://wileyonlinelibrary.com) and [www.ion.org](http://www.ion.org)]

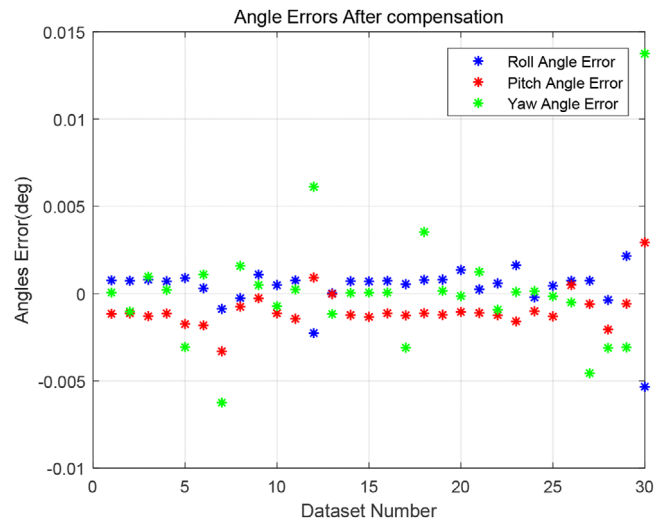


**FIGURE 5** Attitude error values with modified calibration parameters at the end of the navigation process [Color figure can be viewed in the online issue, which is available at [wileyonlinelibrary.com](http://wileyonlinelibrary.com) and [www.ion.org](http://www.ion.org)]

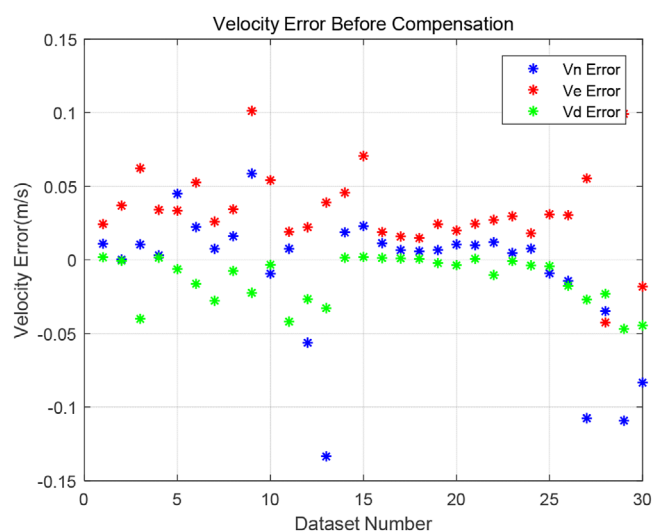


**FIGURE 4** Velocity error value with initial calibration parameters at the end of the navigation process for 30 datasets each with three velocities [Color figure can be viewed in the online issue, which is available at [wileyonlinelibrary.com](http://wileyonlinelibrary.com) and [www.ion.org](http://www.ion.org)]

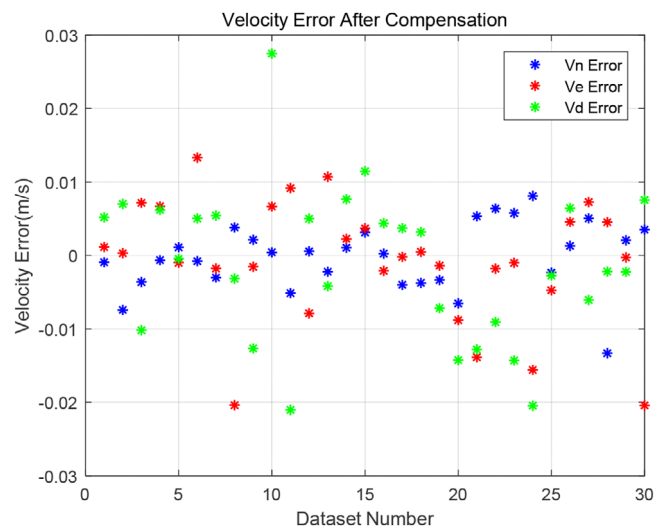


**FIGURE 6** Velocity error values with modified calibration parameters at the end of the navigation process [Color figure can be viewed in the online issue, which is available at [wileyonlinelibrary.com](http://wileyonlinelibrary.com) and [www.ion.org](http://www.ion.org)]

The values of velocity errors with the initial calibration parameters are given in Figure 4.

In the next step, the datasets along with the initial calibration parameters and the exact values of the initial and final states are applied to the algorithm. The full convergence of the calibration parameters is proposed for at least 600 times of running the algorithm with only 1% of the correction parameters at a time. The attitude error values are shown in Figure 5.

The velocity error values are shown in Figure 6.

The accelerometers bias convergence curve is shown in Figure 7.

The gyroscopes bias convergence curve is shown in Figure 8.

The lever arm effect convergence curve is shown in Figure 9.

To evaluate the improved parameters, a 600-second dataset of the system with different movements is stored, and the navigation is performed on it by using the initial and improved calibration parameters.

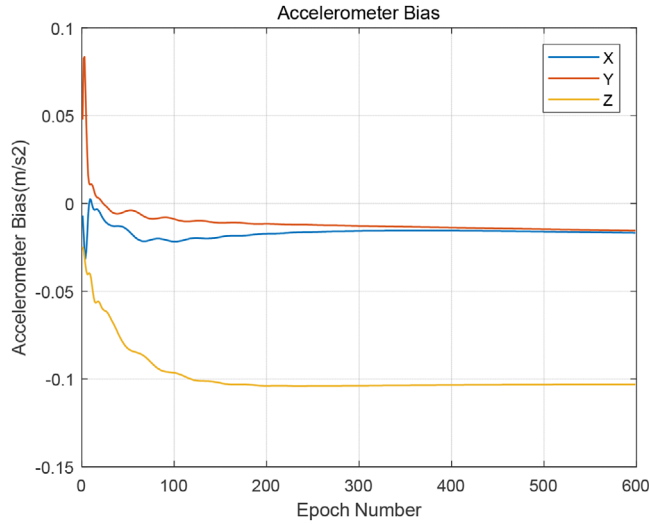


**FIGURE 7** The accelerometers bias convergence curve in calibration procedure. At 600 times running the algorithm, the gyroscopes bias converges after an initial overshoot [Color figure can be viewed in the online issue, which is available at [wileyonlinelibrary.com](http://wileyonlinelibrary.com) and [www.ion.org](http://www.ion.org)]

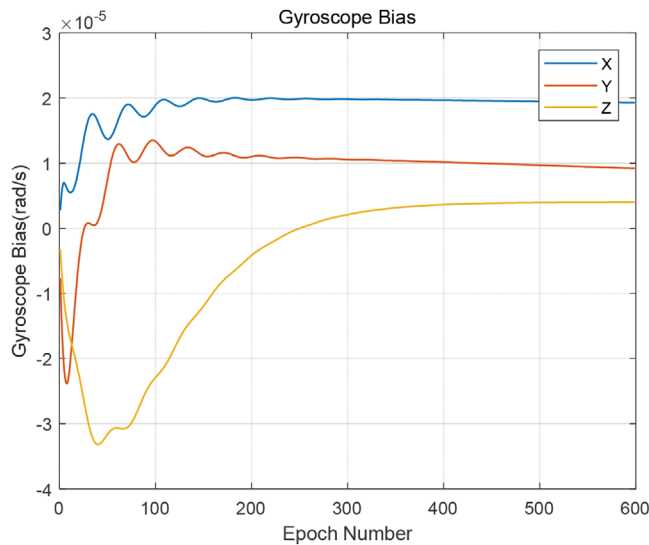


**FIGURE 8** The gyroscopes bias convergence curve in calibration procedure. At 600 times running the algorithm, the gyroscopes bias converges after an initial overshoot [Color figure can be viewed in the online issue, which is available at [wileyonlinelibrary.com](http://wileyonlinelibrary.com) and [www.ion.org](http://www.ion.org)]

In order to simulate the designed algorithm, there is a need for a model of sea turbulence. Different models have been suggested for this purpose in different papers. The models in some papers are presented, for example, in Gu et al. (2008); it is assumed that the ship is in an anchorage and the angles of its heading, pitch, and rolling are changed

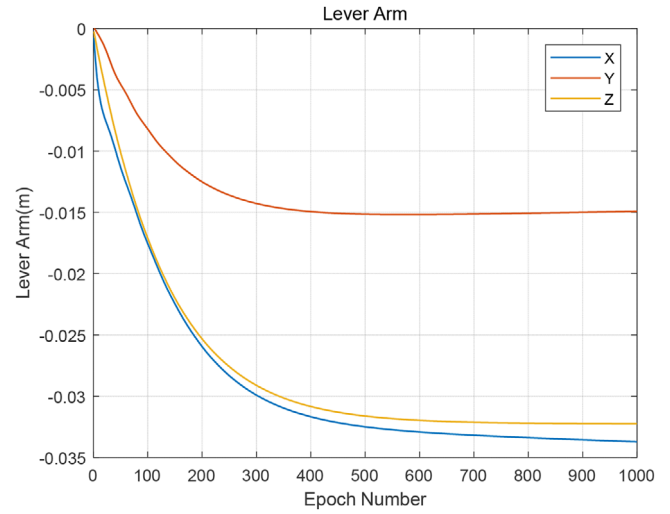


**FIGURE 9** The lever arm effect convergence curve in calibration procedure. With the analysis of the system mechanics and the location of the accelerometers, it can be concluded that the values of the parameters calculated for the lever arm are also reasonable [Color figure can be viewed in the online issue, which is available at [wileyonlinelibrary.com](http://wileyonlinelibrary.com) and [www.ion.org](http://www.ion.org)]

as follows:

$$\begin{aligned}\psi &= 5^\circ \cos\left(\frac{2\pi}{7}t\right) \\ \theta &= 7^\circ \cos\left(\frac{2\pi}{5}t\right) \\ \phi &= 10^\circ \cos\left(\frac{2\pi}{6}t\right),\end{aligned}\quad (30)$$

where  $\psi$  is the heading angle,  $\theta$  is the pitch angle, and  $\phi$  is the roll angle.

The velocity error values for the two states are shown in Figures 10 and 11.

Given the existence of the precise state as a criterion, the analysis of the data and the curves indicate that there is a good improvement in the results. The percentage of velocity error after the compensation of the calibration is 15 percent of the previous error. These noisy areas are due to the movements applied to the IMU. These movements are the simulation of the sea conditions. These noisy areas are also present in Figure 10, but are not clear due to the large error.

From the analysis of the system mechanics and the location of the accelerometers, it can be concluded that the values of the parameters calculated for the lever arm are also reasonable.

The problem of using inaccurate calibration equipment in the weights of the least squares error method can be investigated. Desired values are considered in the proposed calibration algorithm, velocities, and direct cosine matrix (DCM) arrays. By reducing the weight of DCM in the least squares error method, the algorithm can be adjusted to

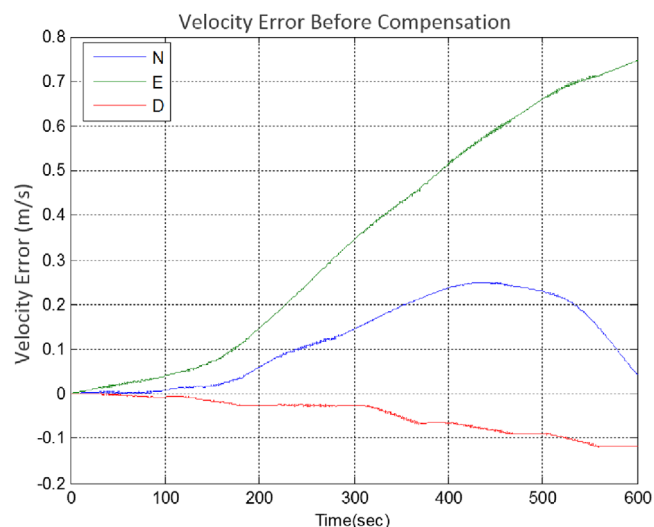


**FIGURE 10** The velocity error curve for 600 seconds of data before using the correction of calibration parameters. The maximum velocity error in 600 seconds is 0.75 m/s. In the proposed algorithm, we want to reduce this error [Color figure can be viewed in the online issue, which is available at [wileyonlinelibrary.com](http://wileyonlinelibrary.com) and [www.ion.org](http://www.ion.org)]

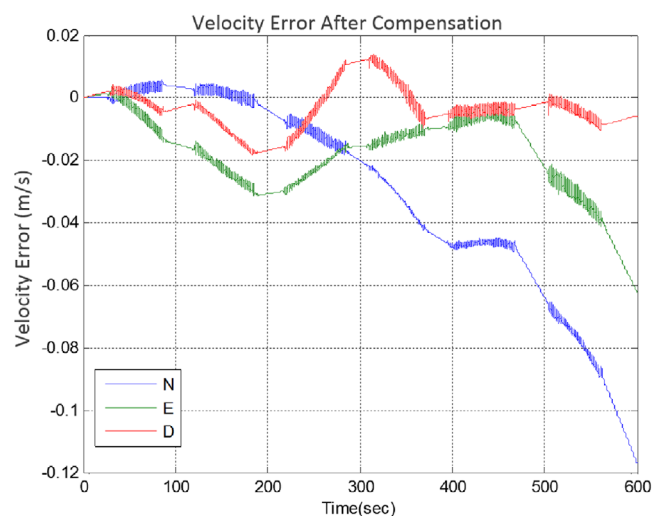


**FIGURE 11** The velocity error curve for 600 seconds of data after using the correction of calibration parameters [Color figure can be viewed in the online issue, which is available at [wileyonlinelibrary.com](http://wileyonlinelibrary.com) and [www.ion.org](http://www.ion.org)]

reduce the effect of attitude and their accuracy. In this case, only zero velocities (also available on inaccurate turn tables) are used as desired values in the least squares error method.

From the tests performed, it is clear that the accuracy of the turn table has no effect on the accuracy of the results of the proposed calibration algorithm because the same weight for velocity values and DCM in the least squares method, due to small numerical values of DCM array error compared to velocity error, virtually eliminates the effect





**FIGURE 12** The K. N. Toosi IMU FOG gyroscopes and Q-FLEX accelerometers (Rahimi & Nikkha, 2020) whose characteristics are detailed in Table 1 [Color figure can be viewed in the online issue, which is available at [wileyonlinelibrary.com](http://wileyonlinelibrary.com) and [www.ion.org](http://www.ion.org)]

of the DCM on the algorithm. In this case, the main effect is related to the velocity error, which is available in inaccurate turn tables.

## 7 | CONCLUSION AND FUTURE WORK

In the event that the existing calibration turn tables do not meet the accuracy requirements of the systems, it is appropriate to use methods that are less dependent on the accuracy of the turn tables. It is difficult to estimate parameters such as the lever arm effect by using conventional separation methods. In this paper, a model was developed for systematic calibration of inertial measurement units, which expresses the rotation matrix and velocity errors as a linear function of calibration parameters at any time and for simple and compound movements. Then, a systematic calibration algorithm was presented using only one specific and precise plate. The proposed algorithm does not have the problems of not fully observing the parameters. Also, in the proposed method, the axes in the calibration are determined on the IMU, based on the mechanical indexes. Using the real data, it was found that the proposed algorithm provides a good estimation of the calibration parameters, and the estimated values of the lever arm parameters correspond to the mechanical structure of the system. For future works, it is recommended to use the magnitude of gravity and rotation rate of Earth as the measurement in static positions. Calibration algorithms can also be developed based on other linear navigation error models such as  $\varphi$  and  $\psi$  models.

## ORCID

Hossein Rahimi  <https://orcid.org/0000-0003-0732-9215>  
Amir Ali Nikkha  <https://orcid.org/0000-0003-1989-6727>

## REFERENCES

- Cai, Q., Yang, G., Song, N., & Liu, Y. (2016). Systematic calibration for ultra-high accuracy inertial measurement units. *Sensors*, 16(6), 940. <https://doi.org/10.3390/s16060940>
- Fu, L., Zhu, Y., Wang, L., & Wang, X. (2011). A D-optimal multi-position calibration method for dynamically tuned gyroscopes. *Chinese Journal of Aeronautics*, 24(2), 210–218. [https://doi.org/10.1016/S1000-9361\(11\)60025-3](https://doi.org/10.1016/S1000-9361(11)60025-3)
- Gu, D., El-Sheimy, N., Hassan, T., & Syed, Z. (2008, May). Coarse alignment for marine SINS using gravity in the inertial frame as a reference. *2008 IEEE/ION Position, Location and Navigation Symposium*, Monterey, CA, 961–965. <https://doi.org/10.1109/PLANS.2008.4570038>
- Hayal, A. G. (2010). *Static calibration of the tactical grade inertial measurement units* (Doctoral dissertation, The Ohio State University). [https://kb.osu.edu/bitstream/handle/1811/78660/1/SES\\_GeodeticScience\\_Report\\_496.pdf](https://kb.osu.edu/bitstream/handle/1811/78660/1/SES_GeodeticScience_Report_496.pdf)
- Hung, C. Y., & Lee, S. C. (2006). A calibration method for six-accelerometer INS. *International Journal of Control, Automation, and Systems*, 4(5), 615–623.
- Kozlov, A., Sazonov, I., & Vavilova, N. (2014, February). IMU calibration on a low grade turntable: Embedded estimation of the instrument displacement from the axis of rotation. *2014 International Symposium on Inertial Sensors and Systems (ISISS)*, Laguna Beach, CA, 1–4. <https://doi.org/10.1109/ISISS.2014.6782525>
- Kozlov, A., Sazonov, I., Vavilova, N., & Parusnikov, N. (2013, May). Calibration of an inertial measurement unit on a low-grade turntable with consideration of spatial offsets of accelerometer proof masses. *Petersburg International Conference on Integrated Navigation Systems*, St. Petersburg, Russia, 126–129.
- Nieminen, T., Kangas, J., Suuriniemi, S., & Kettunen, L. (2010). An enhanced multi-position calibration method for consumer-grade inertial measurement units applied and tested. *Measurement Science and Technology*, 21(10), 105204. <https://doi.org/10.1088/0957-0233/21/10/105204>
- Pan, J., Zhang, C., & Cai, Q. (2014). An accurate calibration method for accelerometer nonlinear scale factor on a low-cost three-axis turntable. *Measurement Science and Technology*, 25(2), 025102. <https://doi.org/10.1088/0957-0233/25/2/025102>
- Parusnikov, N. A. (2009). Bench calibration problem for a strapdown inertial navigation system. *Mechanics of Solids*, 44(4), 497–501. <https://doi.org/10.3103/S0025654409040013>
- Rahimi, H., & Nikkhah, A. A. (2020). Improving the speed of initial alignment for marine strapdown inertial navigation systems using heading control signal feedback in extended Kalman filter. *International Journal of Advanced Robotic Systems*, 17(1). <https://doi.org/10.1177/1729881419894849>
- Rogers, R. M. (2007). *Applied mathematics in integrated navigation systems*. American Institute of Aeronautics and Astronautics.
- Salychev, O. S. (1998). *Inertial systems in navigation and geophysics* (pp. 11–98). Bauman MSTU Press.
- Salychev, O. S. (2004). *Applied inertial navigation: Problems and solutions* (pp. 191–209). BMSTU press.
- Särkkä, O., Nieminen, T., Suuriniemi, S., & Kettunen, L. (2017). A multi-position calibration method for consumer-grade accelerometers, gyroscopes, and magnetometers to field conditions. *IEEE Sensors Journal*, 17(11), 3470–3481. <https://doi.org/10.1109/JSEN.2017.2694488>
- Shin, E. H., & El-Sheimy, N. (2002). A new calibration method for strapdown inertial navigation systems. *Z. vermess*, 127, 1–10.
- Syed, Z. F., Aggarwal, P., Goodall, C., Niu, X., & El-Sheimy, N. (2007). A new multi-position calibration method for MEMS inertial navigation systems. *Measurement Science and Technology*, 18(7), 1897. <https://doi.org/10.1088/0957-0233/18/7/016>
- Titterton, D., Weston, J. L., & Weston, J. (2004). *Strapdown inertial navigation technology* (Vol. 17). IET.
- Vavilova, N. B., & Sazonov, I. Y. (2012). Calibration of a ready-mounted strapdown inertial navigation system on a low-accuracy turntable with one degree of freedom. *Moscow University Mechanics Bulletin*, 67(4), 96–98. <https://doi.org/10.3103/S0027133012040048>
- Xie, B., Qin, Y., & Wan, Y. (2010, June). A high-accuracy calibration method of optical gyro SINS. *2010 3rd International Symposium on Systems and Control in Aeronautics and Astronautics*, Harbin, China, 507–511. <https://doi.org/10.1109/ISSCAA.2010.5633184>
- Zhang, H., Wu, Y., Wu, M., Hu, X., & Zha, Y. (2008, August). A multi-position calibration algorithm for inertial measurement units. *AIAA guidance, navigation and control conference and exhibit*, Honolulu, HI, 7437. <https://doi.org/10.2514/6.2008-7437>

**How to cite this article:** Rahimi H, Nikkhah AA. Improving the calibration process of inertial measurement unit for marine applications. *NAVIGATION*. 2020;67:763–774. <https://doi.org/10.1002/navi.400>